S. F. Leitman, G. Vilaire, D. B. Cines, *Proc. Natl. Acad. Sci. U.S.A.* **80**, 2417 (1983); D. Pidard, R. R. Montgomery, J. S. Bennett, T. J. Kunicki, *J. Biol. Chem.* **258**, 12,582 (1983); B. S. Coller, E. I. Peerschke, L. E. Scudder, C. A. Sullivan, *J. Clin. Invest.* **72**, 325 (1983); Z. M. Ruggieri, L. De Marco, L. Gatti, R. Bader, R. R. Montgomery, *ibid.*, p. 1; E. F. Plow *et al.*, *Blood* **66**, 724 (1985).
13. D. R. Phillips and P. P. Agin, *J. Clin. Invest.* **60**, 535 (1977); J. S. Bennett and G. Vilaire, *ibid.* **64**, 1393 (1979); M. H. Ginsberg, J. Forsyth, A. Lightsey, J. Chediak, E. F. Plow, *ibid.* **71**, 619 (1983); Z. M. Ruggieri, R. Bader, L. DeMarco, *Proc. Natl. Acad. Sci. U.S.A.* **79**, 6038 (1982).
14. G. Pietu, G. Cherel, G. Marguerie, D. Meyer, *Nature (London)* **308**, 648 (1984); E. F. Plow, G. A. Marguerie, M. H. Ginsberg, *Blood*, in press; J. Schullek, J. Jordan, R. R. Montgomery, *J. Clin. Invest.* **73**, 421 (1984).
15. E. F. Plow, A. H. Srouji, D. Meyer, G. Marguerie, M. H. Ginsberg, *J. Biol. Chem.* **259**, 5388 (1984); S. Timmons, M. Kloczewiak, J. Hawiger, *Proc. Natl. Acad. Sci. U.S.A.* **81**, 4935 (1984).
16. J. E. Sadler *et al.*, *Proc. Natl. Acad. Sci. U.S.A.* **82**, 6394 (1985).
17. E. F. Plow, R. Wolff, M. H. Ginsberg, *Thromb. Hemostas.* **54**, 63 (1985).
18. L. Hood, H. V. Huang, W. J. Dreyer, *J. Supramol. Struct.* **7**, 531 (1977).
19. U. K. Laemmli, *Nature (London)* **227**, 680 (1970).
20. E. Engvall and E. Ruoslahti, *Int. J. Cancer* **20**, 1 (1977).
21. E. G. Hayman *et al.*, *Proc. Natl. Acad. Sci. U.S.A.* **80**, 4003 (1983).
22. R. F. Doolittle, D. Schubert, S. A. Schwartz, *Arch. Biochem. Biophys.* **118**, 456 (1967).
23. J. Wencel-Drake, E. F. Plow, T. S. Zimmerman, R. G. Painter, M. H. Ginsberg, *Am. J. Pathol.* **115**, 156 (1984).
24. M. D. Pierschbacher, E. H. Hayman, E. Ruoslahti, *Cell* **26**, 259 (1981).
25. J. M. Gardner and R. O. Hynes, *Cell* **42**, 439 (1985).
26. We thank B. Coller for the generous gift of monoclonal antibody 10E5. Supported by grants HL26838, CA38352, HL28235, HL16411, and Cancer Center support grant CA30199 from the National Institutes of Health.

1 August 1985; accepted 15 November 1985

Distribution of Protein and RNA in the 30*S* Ribosomal Subunit

V. RAMAKRISHNAN

In *Escherichia coli*, the small ribosomal subunit has a sedimentation coefficient of 30*S*, and consists of a 16*S* RNA molecule of 1541 nucleotides complexed with 21 proteins. Over the last few years, a controversy has emerged regarding the spatial distribution of RNA and protein in the 30*S* subunit. Contrast variation with neutron scattering was used to suggest that the RNA was located in a central core of the subunit and the proteins mainly in the periphery, with virtually no separation between the centers of mass of protein and RNA. However, these findings are incompatible with the results of efforts to locate individual ribosomal proteins by immune electron microscopy and triangulation with interprotein distance measurements. The conflict between these two views is resolved in this report of small-angle neutron scattering measurements on 30*S* subunits with and without protein S1, and on subunits reconstituted from deuterated 16*S* RNA and unlabeled proteins. The results show that (i) the proteins and RNA are intermingled, with neither component dominating at the core or the periphery, and (ii) the spatial distribution of protein and RNA is asymmetrical, with a separation between their centers of mass of about 25 angstroms.

THE TECHNIQUE OF CONTRAST VARIation in neutron scattering has been particularly useful in the study of ribosome structure because of the different scattering length densities of protein and nucleic acid. For a particle of volume V the forward scattered intensity $I(0)$ and amplitude $A(0)$, and the radius of gyration R_g are functions of the contrast $\bar{\rho} = \rho_p - \rho_s$ between the mean scattering length density ρ_p of the particle and the scattering length density ρ_s of the solvent (*1*):

$$I(0) = [A(0)]^2 = (\bar{\rho} V)^2 \quad (1)$$

and

$$R_g^2 = R_c^2 + \frac{\alpha}{\bar{\rho}} - \frac{\beta}{\bar{\rho}^2} \quad (2)$$

Here R_c is the radius of gyration of a homogeneous particle that has the same shape as the particle under consideration. The parameter α is the second moment of the fluctuation of the scattering length density of the particle about its mean density, which indicates whether the core of the particle is more or less dense than the periphery. In a two-component system, β is related to the separation d between the centers of mass of the two components by the relation

$$d = \sqrt{\beta}\left(\frac{1}{|\bar{\rho}_1|} + \frac{1}{|\bar{\rho}_2|}\right)$$

where $\bar{\rho}_1$ and $\bar{\rho}_2$ are the contrasts of the particle at which the two components are matched by the solvent (*2*).

Contrast variation has been used to show that in the 30*S* ribosomal subunit, the protein R_g is about 80 Å, the RNA is about 61 to 66 Å, with a value of about -1×10^{-3} for α, and a negligible value of β (*3–6*). These results have led to a model of the small subunit in which the RNA primarily occupies a central core region, with the proteins lying uniformly on the outside. Over the last decade, however, individual proteins have been located on the subunit by the triangulation of measured interprotein distances (*7*) and immune electron microscopy (*8, 9*). These measurements indicate that the radius of gyration of the protein component is 68 Å and that the proteins are not uniformly distributed about the RNA in the 30*S* subunit. This report describes a series of experiments to resolve the conflict between these contradictory views of the structure of the 30*S* ribosomal subunit.

Unlabeled and deuterated 16*S* RNA, 30*S* ribosomal subunits, and subunits reconstituted from deuterated RNA and unlabeled proteins were prepared (*10*). Subunits depleted of protein S1 were prepared by the method of Steitz *et al.* (*11*). All subunits studied were fully active in polyuridylic acid–directed phenylalanine incorporation (*12*). The subunits were characterized on gels (Fig. 1). Scattering measurements were

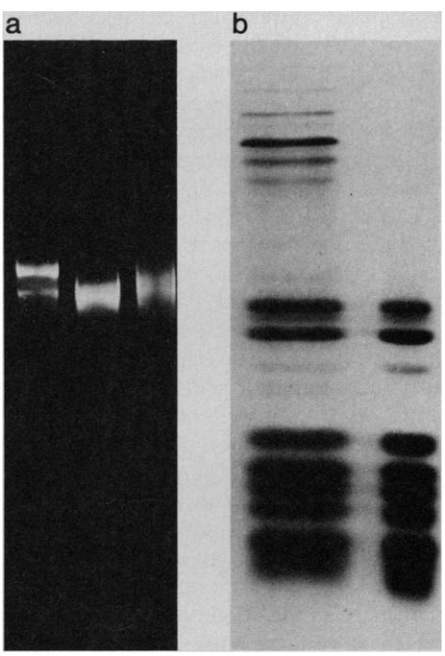

Fig. 1. Ribosomal subunits used for neutron scattering. (a) Gels of 3 percent polyacrylamide, 0.5 percent agarose on the different species studied. Lane 1, 30*S* subunits without salt wash; lane 2, S1-depleted 30*S* subunits; lane 3, 30*S* reconstituted from deuterated 16*S* RNA. (b) Sodium dodecyl sulfate gels (15 percent) on 30*S* ribosomal proteins. Lane 1, subunits with protein S1; lane 2, reconstituted subunits.

Biology Deparment, Brookhaven National Laboratory, Upton, NY 11973.

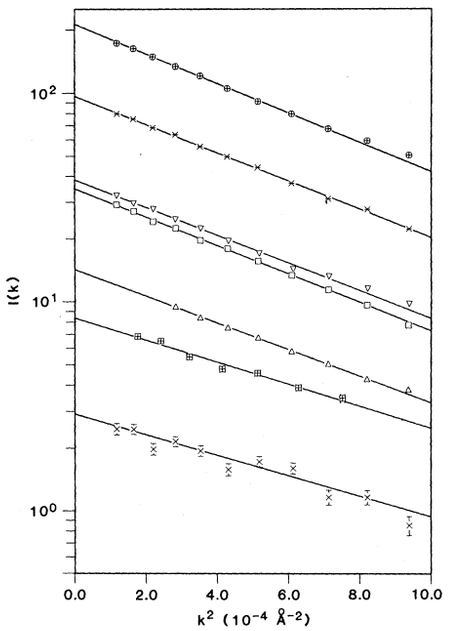

Fig. 2. Guinier plots of data on 30*S* subunits reconstituted from deuterated RNA and unlabeled proteins. Symbols: ⊕, H_2O; *, 23 percent D_2O; ▽, 40 percent D_2O; □, 99.5 percent D_2O; △, 90 percent D_2O; ⊞, 60 percent D_2O; ×, 78 percent D_2O.

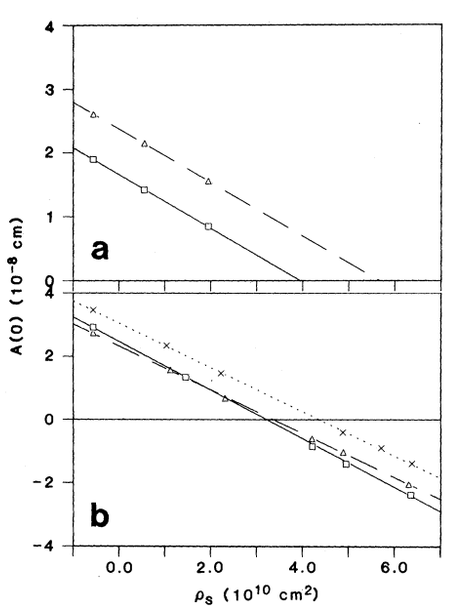

Fig. 3. Match-points for RNA and 30*S* subunits. The forward scattering amplitude $A(0)$ was calculated by taking the square root of the normalized forward scatter $I(0)$. This was plotted against the solvent scattering density, which can be calculated from the mole fraction of D_2O in the sample. (a) □, unlabeled 16*S* RNA; △, deuterated 16*S* RNA. The slopes are identical within error, indicating that the volumes are the same. (b) Data for 30*S* subunits: □, with protein S1 and without salt wash; △, salt-washed to remove S1; ×, reconstituted from deuterated 16*S* RNA and unlabeled proteins.

done in 10 m*M* tris, 50 m*M* KCl, 0.5 m*M* Mg^{2+}, *p*H 7.5, except for free 16*S* RNA, which was studied in reconstitution buffer (10 m*M* tris, 0.3*M* KCl, 10 m*M* Mg^{2+}). Data were collected on the H9B spectrometer (*13*) at the High Flux Beam Reactor at Brookhaven National Laboratory. Measurements were made at different solvent H_2O:D_2O ratios. Guinier plots of typical scattering data are shown in Fig. 2.

The radius of gyration R_g and forward scatter $I(0)$ were calculated from Guinier plots of the data, and the match-points were determined by a plot of the forward scattering amplitude $A(0)$ against the solvent density (Fig. 3). The slope of this plot is proportional to the molecular volume, and the match-point is a function of the degree of deuteration (*1*). When this treatment is applied to the curves for deuterated and unlabeled 16*S* RNA with the assumption that about 80 percent of the noncarbon-bonded hydrogens in the RNA are exchangeable (*14*), one can calculate a partial specific volume of 0.579 cm^3/g and a degree of deuteration of 58.6 percent of carbon-bonded hydrogens.

Information about the protein and RNA components of the subunit is obtained by an analysis of Stuhrmann plots of the data (R_g^2 versus $1/\bar{\rho}$). These plots show that for 30*S* subunits that were not salt-washed (Fig. 4a), the data resemble those previously published, yielding a protein-dominated R_g of 81 Å, an RNA-dominated R_g of 62 Å, and a value for α of $-1.1 \times/10^{-3}$. On the other hand, the plot for subunits depleted of S1 and any adventitiously bound nonribosomal proteins (Fig. 4b) showed a negligible slope α, with an R_g of 68 to 70 Å for both protein and RNA. In both of these cases, the value of the reduced χ^2 was not improved by a parabolic rather than a linear fit, showing that the parameter β was small.

However, when one enhances the contrast between RNA and protein by selective deuteration, a different result is obtained. Data for 30*S* subunits reconstituted from deuterated RNA and unlabeled proteins show a distinct curvature of the Stuhrmann plot (Fig. 4c), with a poor fit to a straight line (reduced $\chi^2 = 11$) but a good fit to a parabola (reduced $\chi^2 = 0.8$), indicating a significant value of β. The value of β estimated from a parabolic fit is $2.9 \pm 0.2 \times 10^6$ cm^{-2}, which corresponds to a separation between the centers of mass of protein and RNA of 25 ± 2 Å. This separation would give rise to a value of 1.0×10^6 cm^{-2} for β in the unlabeled subunit. As can be seen by the dashed line in Fig. 4b, the measured data are compatible with this value of β, with a reduced χ^2 of 1.9, compared with 1.6 for $\beta = 0$. However, the natural density difference between protein and RNA is insufficient to measure accurately a separation of 25 Å between their centers of mass in the 30*S* ribosome.

The negligible value of α shows that the protein and RNA are intermingled in the region of overlap, with neither component dominating the core or the periphery. The radius of gyration of free 16*S* RNA in reconstitution buffer is 90 Å and is independent of contrast. This value is much higher than the value in the subunit, confirming the results of Serdyuk *et al.* (*15*) that 16*S* RNA condenses upon binding of ribosomal proteins. The intermingling of proteins and RNA in the subunit suggests therefore that 16*S* RNA has binding sites for proteins located well within its interior. The relatively extended structure of free 16*S* RNA is

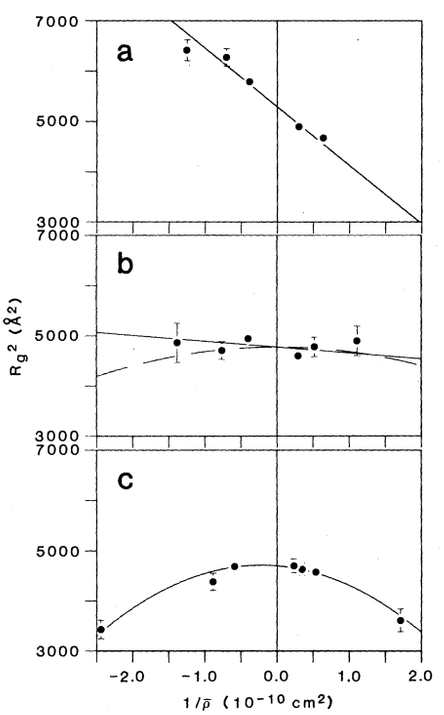

Fig. 4. Stuhrmann plots (R_g^2 versus $1/\bar{\rho}$) for 30*S* ribosomal subunits: (a) subunits that were not salt-washed; (b) subunits that were salt-washed to remove S1; (c) subunits that were reconstituted from deuterated 16*S* RNA and unlabeled proteins. In all cases, the data points were fitted to a straight line or a parabola. In (a) and (b), a parabolic fit was no better than a linear fit. In (c) a parabolic fit was significantly better than a linear fit, which is also apparent from the curvature of the data points. The best fit in each case is shown by the solid curve. The center of mass separation between RNA and protein can be calculated from the parabolic term in (c). Calculation of the expected parabola for this center of mass separation for an unlabeled 30*S* subunit (without S1) gives rise to the dashed curve in (b), showing that the measured data are compatible with this separation, but that the natural contrast between unlabeled RNA and protein gives rise to a curvature too small to measure.

evidence that these sites are initially open and accessible, but that compaction of the complex occurs upon binding of ribosomal proteins.

It is not clear why Stuhrmann plots for non–salt-washed subunits have such a large slope and a consequently large value of the protein R_g while subunits salt-washed to remove protein S1 do not. It is unlikely that the S1-depleted and reconstituted species studied here have suffered a partial loss of ribosomal proteins, because both of these species are fully active and have measured contrast match-points that are identical within error to calculated values. S1 has been located close to the protein center of mass (*16*) and therefore should not make a large difference to the protein R_g. Sodium dodecyl sulfate gels (Fig. 1b) on the subunits with S1 show the presence of several bands corresponding to nonribosomal proteins that are not present in the salt-washed or reconstituted subunits. The match-point for the subunits with S1 is also slightly lower than calculated; this leads to an estimate of about 11 percent more protein than would be expected from a unit stoichiometry of the 21 ribosomal proteins. Thus it is likely that nonribosomal proteins are bound to the region of RNA that is farthest from the protein center of mass, giving rise to a spuriously large R_g for the protein component. On the other hand, in at least one previous report (*6*), the subunits studied were washed in 0.5*M* NH_4Cl. The possibility remains, therefore, that the location of S1, which was determined by measuring the distance of cross-linked S1 to other ribosomal proteins, is erroneous.

In any case, with the possible exception of protein S1, the proteins and RNA of the 30*S* ribosomal subunit are intermingled, but are asymmetric in their spatial distribution, with a center of mass separation of 25 Å. These findings offer direct and independent evidence that the picture of the small subunit that is emerging from efforts to locate individual ribosomal proteins is correct with respect to the overall distribution of protein and RNA.

REFERENCES AND NOTES

1. K. Ibel and H. B. Stuhrmann, *J. Mol. Biol.* **93**, 255 (1975).
2. M. H. J. Koch and H. B. Stuhrmann, *Methods Enzymol.* **59**, 670 (1979).
3. P. B. Moore, D. M. Engelman, B. P. Schoenborn, *J. Mol. Biol.* **91**, 101 (1975).
4. P. Beaudry, H. U. Petersen, M. Grunberg-Manago, B. Jacrot, *Biochem. Biophys. Res. Commun.* **72**, 391 (1976).
5. H. B. Stuhrmann *et al.*, *J. Mol. Biol.* **119**, 203 (1978).
6. I. N. Serdyuk, A. K. Grenader, G. Zaccai, *ibid.* **135**, 691 (1979).
7. P. B. Moore *et al.*, in *Structure, Function and Genetics of Ribosomes*, B. Hardesty, Ed. (Springer, New York, in press).
8. L. Kahan, D. A. Winkelmann, J. A. Lake, *J. Mol. Biol.* **145**, 193 (1981).
9. B. Kastner, M. Noah, M. Stoffler-Meilicke, G. Stoffler, *Proc. 10th Int. Congr. Electron. Microsc.* **93**, 99 (1983).
10. P. B. Moore, *Methods Enzymol.* **59**, 639 (1979).
11. J. A. Steitz, A. J. Wahba, M. Laughrea, P. B. Moore, *Nucleic Acids Res.* **4**, 1 (1977).
12. R. F. Gesteland, *J. Mol. Biol.* **18**, 356 (1966).
13. D. Schneider and B. P. Schoenborn, in *Neutrons in Biology*, B. P. Schoenborn, Ed. (Plenum, New York, 1984), pp. 119–142.
14. S. I. Edelstein and H. K. Schachman, *Methods Enzymol.* **27**, 82 (1973).
15. I. Serdyuk *et al.*, *J. Mol. Biol.* **169**, 409 (1983).
16. I. Y. Sillers and P. B. Moore, *ibid.* **153**, 761 (1981).

17. Research was carried out under the auspices of the U.S. Department of Energy. I thank D. Schneider for his help with these experiments, P. B. Moore for a gift of deuterated RNA, and B. P. Schoenborn for his encouragement. I thank R. M. Sweet for a critical reading of this manuscript.

12 August 1985; accepted 16 December 1985

Calcium Channels in Planar Lipid Bilayers: Insights into Mechanisms of Ion Permeation and Gating

ROBERT L. ROSENBERG, PETER HESS, JOHN P. REEVES, HENRY SMILOWITZ, RICHARD W. TSIEN

Electrophysiological recordings were used to analyze single calcium channels in planar lipid bilayers after membranes from bovine cardiac sarcolemmal vesicles had been incorporated into the bilayer. In these cell-free conditions, channels in the bilayer showed unitary barium or calcium conductances, gating kinetics, and pharmacological responses that were similar to dihydropyridine-sensitive calcium channels in intact cells. The open channel current varied in a nonlinear manner with voltage under asymmetric (that is, physiological) ionic conditions. However, with identical solutions on both sides of the bilayer, the current-voltage relation was linear. In matched experiments, calcium channels from skeletal muscle T-tubules differed significantly from cardiac calcium channels in their conductance properties and gating kinetics.

CALCIUM CHANNELS ARE VITAL TO neurotransmission, secretion, and muscle contraction and are important targets of neurochemical modulators (*1*). The molecular properties of Ca^{2+} channels have been studied with single-channel recordings in intact cells (*2–6*) and with biochemical investigations of putative Ca^{2+} channel proteins (*7*). These different approaches to channel function and structure can be combined by studying Ca^{2+} channels under cell-free conditions where the lipid and ionic environment can be controlled. This can be done by recording the activity of Ca^{2+} channels incorporated into planar bilayers (*8–10*). However, there has been no direct comparison of single-channel properties in planar bilayers and in intact cells under matched experimental conditions. Here we report that cardiac Ca^{2+} channels reconstituted in artificial membranes and Ca^{2+} channels in intact heart cells have similar properties of ion permeation and gating. We have also been able to gain new information about the mechanism of ion permeation by using this technique to study calcium channels under experimental conditions unattainable in intact cells. Furthermore, we find that Ca^{2+} channels from skeletal muscle T tubules and cardiac sarcolemma differ significantly in single-channel conductance and gating despite their common sensitivity to dihydropyridines.

Unitary Ca^{2+} channel activity was observed after incorporation of cardiac sarcolemmal vesicles into a lipid bilayer (Fig. 1A) (*11*). The external side to the channel was exposed to 100 m*M* Ba^{2+} and 50 m*M* Na^+ and the internal side to 50 m*M* Na^+ and no Ba^{2+}. In these studies, channel sidedness is defined such that positive internal potentials promote channel openings (*12*). The dihydropyridine (DHP) Ca^{2+} agonist Bay K 8644 (*13*) was included in all experiments to promote long openings of L-type Ca^{2+} channels (*6, 14, 15*). Membrane depolarizations to +10 mV evoked channel activity (Fig. 1A) that was seen as inward current pulses of ~1.2 pA. This current must have been carried by Ba^{2+} ions because Ba^{2+} was the only ion present that had an inwardly directed driving force at +10 mV. The slope conductance at 0 mV was 23 picosiemens (pS). In experiments with 100 m*M* external Ca^{2+}, unitary current events at +10 mV were only ~0.4 pA, and the slope conductance was ~7 pS. These amplitudes of elementary currents are typical for cardiac L-type Ca^{2+} channels in cell-attached patches (*3, 5, 15*).

R. L. Rosenberg, P. Hess, R. W. Tsien, Department of Physiology, Yale University School of Medicine, New Haven, CT 06510.
J. P. Reeves, Roche Institute of Molecular Biology, Nutley, NJ 07110.
H. Smilowitz, Department of Biochemistry, University of Connecticut, Farmington, CT 06032.